

# The Probability Distribution of Daily Precipitation at the Point and Catchment Scales in the United States

Lei Ye<sup>1\*</sup>, Lars S. Hanson<sup>2</sup>, Pengqi Ding<sup>1</sup>, Dingbao Wang<sup>3</sup>, Richard M. Vogel<sup>4</sup>

<sup>1</sup> School of Hydraulic Engineering, Dalian University of Technology, Dalian, China

<sup>2</sup> Institute for Public Research, Center for Naval Analyses, Arlington, Virginia, USA.

<sup>3</sup> Department of Civil, Environmental, and Construction Engineering, University of Central Florida, Orlando, Florida, USA

<sup>4</sup> Department of Civil and Environmental Engineering, Tufts University, Medford, Massachusetts, USA

**Abstract:** Choosing a probability distribution to represent daily precipitation depths is important for precipitation frequency analysis, stochastic precipitation modeling and in climate trend assessments. Early studies identified the 2-parameter Gamma (G2) distribution as a suitable distribution for wet-day precipitation based on the traditional goodness of fit tests. Here, probability plot correlation coefficients and L-moment diagrams are used to examine distributional alternatives for the wet-day series of daily precipitation for hundreds of stations at the point and catchment scales in the United States. Importantly, both Pearson Type-III (P3) and Kappa (KAP) distributions perform very well particularly for point rainfall. Our analysis indicates that the KAP distribution best describes the distribution of wet-day precipitation at the point scale, whereas the performance of G2 and P3 distributions are comparable for wet-day precipitation at the catchment scale, with P3 generally providing the improved goodness of fit over G2. Since the G2 distribution is currently the most widely used probability density function, our findings could be considerably important, especially within the context of climate change investigations.

**Key Words:** Climate; Rainfall; Weather; L-moment diagram; PPCC; Pearson type III; Kappa; Gamma; Wet-day; Frequency analysis; Trend detection; Stochastic weather models

## 1. Introduction

Precipitation is paramount in the fields of hydrology, meteorology, climatology, and others. However, long series of precipitation data are not always available; therefore, establishing a probability distribution that provides a good fit to daily precipitation depths has long been a topic interest. Investigations into the probability distribution of daily precipitation can be found in at least three main research areas, namely, (1) stochastic precipitation models, (2) frequency analysis of precipitation, and (3) precipitation trends related to global climate change. Table 1 displays a sampling of the literature related to those three topics including the particular precipitation series and durations under investigation, and the proposed probability distributions recommended. Table 1 is by no means exhaustive; it only attempts to document the widespread interest in the

---

\* Corresponding author. E-mail address: yelei@dlut.edu.cn

43 determination of a suitable distribution for daily precipitation totals in a wide range of  
44 studies across a wide range of fields of inquiry.

45 *[Table 1 goes here]*

## 46 **1.1 Stochastic precipitation models**

47 Our central goal is to select a suitable generalized probability distribution for modeling  
48 daily precipitation depths, thus we are only concerned with the class of “two-part”  
49 stochastic daily precipitation models that utilize a probability distribution function to  
50 describe precipitation amounts on wet-days, while a probabilistic representation of  
51 precipitation occurrences can be separately described using a Markov model or some  
52 form of a stochastic renewal process (Buishand, 1978; Geng et al., 1986; Waymire and  
53 Gupta, 1981; Watterson, 2005). We only consider the selection of a suitable distribution  
54 for modeling wet-day daily rainfall, leaving the stochastic representation of the  
55 occurrence of zeros, to others.

56 It is evident from Table 1 that the wet-day precipitation series is the primary  
57 series considered within the stochastic precipitation model literature. Thom’s (1951)  
58 suggestion of the 2-parameter Gamma (G2) distribution function for wet-day amounts  
59 seems to carry considerable weight. Buishand (1978) lent support to the suggestion of  
60 the G2 distribution by showing that for the wet-day series at six stations, the empirical  
61 Coefficient of Variation to Coefficient of Skewness ratio was quite close to the  
62 theoretical value of two for a G2 distribution. Geng et al. (1986) provided a review of  
63 other literature supporting the use of the G2 distribution for modeling wet-day rainfall.

64 While the G2 distribution is by far the most commonly advocated distribution for  
65 wet-day precipitation amounts, other distributions have also been suggested. Woolhiser  
66 and Roldan (1982), Wilks (1998) and Li et al. (2013) suggested the use of a three-  
67 parameter mixed exponential distribution instead of G2. Through a variety of goodness  
68 of fit tests and log-likelihood analyses, the mixed exponential was preferred to G2 (Wilks,  
69 1998).

70 The Weibull (W2) and to a lesser extent the exponential distribution have also  
71 been suggested for modeling daily precipitation amounts (Duan et al., 1995; Burgueno et  
72 al., 2005). Duan et al. (1995) used a Chi-squared test to demonstrate that synthetic  
73 rainfall generated from the W2 and G2 models best match the observed daily rainfall data  
74 within each month. Burgueno et al. (2005) used graphical methods and the Kolmogorov-  
75 Smirnov test to give support to the W2 and exponential distributions.

## 76 **1.2 Precipitation frequency analysis**

77 The second section of Table 1 displays a small portion of the literature related to  
78 precipitation frequency analyses. Since extreme rainfall values are of primary  
79 importance in these studies, censored series of rainfall (e.g. the Annual Maximum Series  
80 (AMS) and Partial Duration Series (PDS)) are often useful in these analyses (Stedinger et  
81 al., 1993). Table 1 displays that many of the precipitation frequency investigations of  
82 daily precipitation depths have selected the AMS series.

83 For many years, the most common approach to summarizing precipitation  
84 frequency analyses in the United States was the work of Hershfield (1961), which is

85 commonly referred to as TP-40. Hershfield (1961) fitted a Gumbel distribution to the  
86 AMS of 24-hour precipitation. In the context of a national revision to the TP-40, Bonnin  
87 et al., (2006) fitted a generalized extreme value (GEV) distribution to the AMS of rainfall.

88 While the results of Bonnin et al. (2006) apply to the United States, other  
89 researchers have found similar results using similar methods in other parts of the world.  
90 Pilon et al. (1991) used L-moment goodness-of-fit results to show that the Gumbel  
91 distribution should be rejected in the favor of the GEV in Ontario, Canada. In Korea,  
92 Park and Jung (2002) successfully used the Kappa distribution (of which the GEV is a  
93 special case) to generate extreme precipitation quantile maps. In perhaps the most  
94 comprehensive assessment of the distribution of precipitation extremes, Papalexioiu and  
95 Koutsoyiannis (2013) examined the goodness-of-fit of the GEV distribution to a global  
96 dataset of AMS. Analysis of such a large dataset enabled them to conclude that GEV  
97 models of AMS of daily precipitation provide a good approximation.

98 Interestingly, while a great deal of attention is given to fitting distributions to the  
99 relatively short AMS series of precipitation depths, very few studies directly explore the  
100 probability distribution of the complete series of daily precipitation (including zeros) or  
101 the wet-day series of daily precipitation (zeros excluded). Shoji and Kitaura (2006)  
102 investigated both complete and wet-day daily precipitation series, but included only the  
103 normal, lognormal, exponential, and W2 distributions as candidate distributions, and did  
104 not employ modern regional hydrologic methods such as the method of L-moments.  
105 Deidda and Puliga (2006) investigated the degree of left-censoring of wet-day series  
106 needed to fit a Generalized Pareto (GPA) distribution for 200 stations in Italy with a  
107 range of modern statistical analysis techniques. Wilson and Toumi (2005) derived a  
108 fundamental distribution for heavy rainfall, with a simple expression for rainfall as the  
109 product of mass flux, specific humidity, and precipitation efficiency. Statistical theory  
110 predicted that the tail of the derived rainfall distribution has a stretched exponential form  
111 with a shape parameter of  $2/3$ , which was verified by a global daily precipitation data set.

112 Perhaps the most thorough investigations, to date, on the probability distribution  
113 of daily precipitation amounts are the global studies by Papalexioiu and Koutsoyiannis  
114 (2012, 2016, 2018). Papalexioiu and Koutsoyiannis (2012) derived a generalized Gamma  
115 distribution (GG) from Entropy theory, using plausible constraints for wet-day series of  
116 daily precipitation series. Together, the two studies by Papalexioiu and Koutsoyiannis  
117 (2012, 2016) revealed that the GG distribution provides a good approximation to the  
118 behavior of observed L-moments of global series of wet-day daily precipitation at 11,519  
119 and 14,157 stations, respectively. Additionally, the GG distribution was also used to  
120 generate gridded daily precipitation that is consistent with monthly observations (see  
121 Figure 11 in Papalexioiu et al. (2018)).

### 122 **1.3 Precipitation trends and changes**

123 The third section of Table 1 summarizes a small portion of the precipitation trend  
124 literature which has become a rather large area of inquiry due to concerns over climate  
125 change, as evidenced from recent reviews on the subject (Easterling et al., 2000;  
126 Trenberth, 2011; Madsen et al., 2014). Almost universally, the G2 distribution appears to  
127 be accepted without serious consideration of alternative distributions. For instance,  
128 Groisman et al. (1999) compared maps of the empirical probability of summer 1-day

129 rainfall exceeding 50.4 mm with maps of probabilities determined by a stochastic model  
130 using the fitted G2 distribution for the amounts. They found acceptable fits in regions  
131 where there are enough observed daily rainfall events greater than 50.4 mm.

132 This is an interesting contrast to the precipitation frequency analysis literature  
133 where a G2 distribution is often fit to wet-day series for the purpose of examining  
134 extreme rainfalls instead of using the AMS series fitted by a GEV or other distribution.  
135 Yoo et al. (2005) explained that conventional frequency analysis (using AMS) cannot  
136 expect to predict precipitation changes resulting from climate change; while an  
137 examination of the differences in the G2 distribution's parameters (fitted to the whole  
138 wet-day record) might predict such changes. They found that modifying the parameters  
139 of the daily G2 distribution can explain changes in rainfall quantiles predicted by General  
140 Circulation Models under various climate change scenarios.

141 In a national study of precipitation trends, Karl and Knight (1998) employed the  
142 G2 distribution to fill in missing precipitation observations. Both Watterson and Dix  
143 (2003) and Watterson (2005) assumed a G2 distribution for daily precipitation in the  
144 development of stochastic rainfall models for use in evaluating changes in precipitation  
145 extremes.

#### 146 **1.4 Research objectives**

147 In summary, there are a wide variety of previous studies which have explored the  
148 probability distribution of daily precipitation for the purposes of precipitation frequency  
149 analysis, stochastic precipitation modeling and for trend detection. There seems to be a  
150 consensus that annual maxima appear to be well approximated by either a GEV or  
151 Gumbel probability density function (pdf); while peaks above threshold values are well  
152 approximated by a GPA distribution, and the series of wet-day precipitation is well  
153 approximated by a G2, GG, W2 or in some cases a mixed exponential distribution.  
154 However, other than the two recent global studies by Papalexiou and Koutsoyiannis  
155 (2012, 2016), we are unaware of any studies that have used recent developments in  
156 regional hydrologic frequency analysis such as L-moment diagrams or probability plot  
157 goodness of fit evaluations to evaluate the probability distribution of very large regional  
158 datasets comprised of the wet-day series of daily precipitation.

159 The recent studies by Papalexiou and Koutsoyiannis (2012; 2016) represent  
160 perhaps the most comprehensive studies to date. However, their L-moment evaluations  
161 only evaluate the relationship between L-Skewness and L-Cv; thus they were unable to  
162 fully evaluate the goodness-of-fit of the several relatively new three-parameter pdfs  
163 introduced in their studies such as the GG and the Burr type XII pdfs which would  
164 require construction of L-Kurtosis versus L-Skew diagrams which are currently  
165 unavailable for those pdfs. Analogous to those two studies, this paper uses two large  
166 scale national datasets to re-examine the question of which of the commonly used  
167 continuous distribution functions which are widely used in the fields of hydrology,  
168 meteorology and climate best fit wet-day series of observed daily precipitation data. We  
169 focus our research interest on the distribution of wet-day series of precipitation since the  
170 pdf of complete series can be derived by a mixed distribution consisting of a combination  
171 of the pdf of wet-day series and a stochastic model of the percentage and occurrence of  
172 zeros.



215 **3.1 L-Moment diagrams**

216 L-moment diagrams are now a widely accepted approach for evaluating the goodness of  
217 fit of alternative distributions to observations. The theory and application of L-moments  
218 introduced by Hosking (1990) are now widely available in the literature (Stedinger et al.,  
219 1993; Hosking and Wallis, 1997), hence it is not reproduced here.

220 The distribution of wet-day series of precipitation is highly skewed due to the  
221 large proportion of small non-zero values and high variance. Higher order conventional  
222 moment ratios such as skewness and kurtosis are very sensitive to extreme values and can  
223 exhibit enormous downward bias even for extremely large sample sizes (Vogel and  
224 Fennessey, 1993) as is the case here. However, L-moment ratios are approximately  
225 unbiased in comparison to conventional moment ratios, thus providing a particularly  
226 useful tool for investigating the pdf of daily wet-day precipitation series.

227 L-moment ratio diagrams provide a convenient graphical image to view the  
228 characteristics of sample data compared to theoretical statistical distributions. The L-  
229 moment diagrams: L-Kurtosis ( $\tau_4$ ) vs L-Skew ( $\tau_3$ ) and L-Cv ( $\tau_2$ ) vs L-Skew ( $\tau_3$ ) enable us  
230 to compare the goodness of fit of a range of four-parameter, three-parameter, two-  
231 parameter, and one-parameter (or special case) distributions. Table 2 displays  
232 distributions analyzed by means of the  $\tau_4$  vs  $\tau_3$  L-moment ratio diagrams.

233 *[Table 2 goes here]*

234 Table 3 displays distributions analyzed by means of the  $\tau_2$  vs  $\tau_3$  L-moment ratio  
235 diagrams.

236 *[Table 3 goes here]*

237 L-moment ratio diagrams have been used before to examine the distribution of  
238 series of annual maximum precipitation data (Pilon et al., 1991; Park and Jung, 2002; Lee  
239 and Maeng, 2003; Papalexiou and Koutsoyiannis, 2013) and left-censored records  
240 (Deidda and Puliga, 2006). Other than the two recent global studies by Papalexiou and  
241 Koutsoyiannis (2012, 2016) which examined the agreement between empirical and  
242 theoretical relationships between L-Cv and L-Skew, this is the only study we are aware  
243 of, in which a set of daily wet-day precipitation records have been subjected to such a  
244 comprehensive L-moment goodness-of-fit analysis. L-moment estimators were chosen in  
245 this study for a variety of reasons: (1) they are easily computed and nicely summarized  
246 by Hosking and Wallis (1997) for all the cases considered in this study, and (2) estimates  
247 of L-moments are unbiased and estimates of L-moment ratios are nearly unbiased, and  
248 thus for the extremely large sample sizes considered here, sampling variability of  
249 empirical L-moment ratios will be extremely small especially when contrasted to the  
250 variability among the theoretical L-moment ratios corresponding to the various  
251 distributions considered..

252 **3.2 Probability plot correlation coefficient goodness-of-fit evaluation**

253 Probability plots are constructed for each of the wet-day series using L-moment  
254 estimators of the distribution parameters (see Hosking and Wallis (1997)) for the  
255 distributions indicated in Table 4. A probability plot is constructed in such a manner as

256 to ensure that the observations will appear to create a linear relationship when they arise  
257 from the hypothesized distribution assumed for each plot.

258 [Table 4 goes here]

259 The goodness of fit of each probability plot is summarized using a probability plot  
260 correlation coefficient (PPCC, or simply,  $r$ ) which is simply a measure of the linearity of  
261 the plot. The PPCC statistic has a maximum value of 1. The PPCC has been shown to be  
262 a powerful statistic for evaluating the goodness-of-fit of a wide range of alternative  
263 distributional hypotheses (Stedinger et al., 1993) and for performing hypothesis tests of  
264 various two parameter distributional alternatives.

265 To construct a probability plot and to estimate a PPCC, requires estimation of a  
266 plotting position. There are two classes of plotting positions, those that yield unbiased  
267 exceedance probabilities and those that yield unbiased quantile estimates. The Weibull  
268 plotting position given by  $p=i/(n+1)$  yields an unbiased estimate of exceedance  
269 probability regardless of the underlying distribution (see Stedinger et al. (1993)).  
270 Alternatively, there would be a unique plotting position to use for each probability  
271 distribution, and it is now well known that unbiased plotting positions for three parameter  
272 distributions require an additional parameter to estimate within the plotting position. For  
273 example, Vogel and McMartin (1991) derived an unbiased plotting position for the P3  
274 distribution which depends upon the skewness of the distribution, a parameter which adds  
275 so much additional uncertainty to the analysis that led Vogel and McMartin (1991), after  
276 considerable analysis, to not recommend its use. To put all the distributional alternatives  
277 on the same footing, we chose to use the Weibull plotting position for estimation of all  
278 PPCC values.

## 279 **4. Results and analysis**

### 280 **4.1 L-Moment Diagrams**

#### 281 **4.1.1 L-Cv vs L-Skew**

282 Figure 4 displays empirical and theoretical distributional relationships between L-Cv and  
283 L-Skew for point values of daily precipitation (Figure 4a) and areal average values of  
284 daily precipitation (Figure 4b). The various curves represent the theoretical relationship  
285 between L-Cv and L-Skew for the distributions indicated. Each plotted point represents  
286 the empirical relationship between L-Cv and L-Skew for a single precipitation station or  
287 catchment. By comparing the empirically derived points with the theoretical curves, it is  
288 possible to see the degree to which the distributional tail behavior of the data record  
289 matches those of the candidate distributions. We emphasize again, importantly, that the  
290 sample sizes are large enough in this study so that one may, approximately, ignore  
291 sampling variability in all L-moment diagrams. This phenomenon was nicely illustrated  
292 in Figure 2 of Blum et al. (2017), using synthetic data, for record lengths similar to those  
293 used here, but corresponding to daily streamflow records.

294 [Figure 4 goes here]

295 In Figure 4a, the L-moment ratios fall primarily within a region bounded by the  
296 G2 and GP2 theoretical curves, with the W2 passing through some of the points. In  
297 Figure 4b, the L-moment ratios fall primarily in the upper region of the W2 theoretical

298 curve, with the G2 passing through or very close to most of the points. These patterns do  
299 not indicate a clearly preferred distribution for point values, especially considering that  
300 the large sample sizes associated with these series result in negligible sampling variability.  
301 However, Figure 4b documents that the G2 pdf provides a good approximation to the pdf  
302 of wet-day series for areal average values.

303 Blum et al. (2017, Figure 2) used L-moment diagrams for complete and synthetic  
304 series of daily streamflow observations to demonstrate that the sampling variability in L-  
305 moment ratios is negligible for the sample sizes considered in this study. Thus, the  
306 scatter shown in Figure 4 is likely due to real distributional differences rather than due to  
307 sampling variability as is often the case when one constructs L-moment diagrams for  
308 short AMS precipitation and streamflow records, as is the case in most previous studies  
309 which have employed L-moment ratio diagrams.

#### 310 **4.1.2 L-Kurtosis vs L-Skew**

311 Figure 5 displays empirical and theoretical distributional relationships between L-  
312 Kurtosis vs L-Skew point values of daily precipitation (Figure 5a) and areal average  
313 values of daily precipitation (Figure 5b). It should be noted that the P3 distribution is the  
314 two-parameter G2 with an additional location parameter which does not affect the shape  
315 characteristics and thus the theoretical curve of P3 shown in Figure 5 is the same as the  
316 G2. The same holds for GPA and GP2 and for LN2 and LN3. The empirical  
317 relationships of plotted points for both wet-day series are very similar to the theoretical  
318 relationship for the P3 distribution. In fact, among the pdfs considered in Figure 5, the  
319 P3 pdf seems to be the only 3-parameter distribution that could possibly fit the wet-day  
320 record data. Although there is a small proportion of points lying outside the P3 curve, the  
321 overall fit is still very striking.

322 It should also be noted that the L-moment ratio estimates for both wet-day series  
323 occupy a space that can be well represented by the KAP distribution, which occupies a  
324 region of the L-Kurtosis vs L-Skew diagram as shown in Figure A1 of Hosking and  
325 Wallis (1997). A complete description of the 4-parameter KAP distribution is referred to  
326 Hosking (1994) and Hosking and Wallis (1997).

327 *[Figure 5 goes here]*

### 328 **4.2 Probability Plot Correlation Coefficient**

#### 329 **4.2.1 Standard boxplots of PPCC**

330 The L-moment ratio diagrams were useful for identifying several potential candidate  
331 distributions for representing the wet-day daily precipitation series at the point and  
332 catchment scales. From that analysis, we conclude that a four parameter Kappa pdf is  
333 needed to approximate the pdf of point wet-day series whereas a G2 and P3 pdf are  
334 adequate to approximate the pdf of areal average wet-day series. The PPCC statistic  
335 offers another quantitative method for comparing the goodness of fit of different  
336 distributions to the daily precipitation observations. Table 5 summarizes the central  
337 tendency and spread of the values of PPCC for each of the distributions for the wet-day  
338 series of point and catchment scale daily precipitation, respectively. The highest values  
339 for the mean, median, 95<sup>th</sup> percentile and 5<sup>th</sup> percentile of the PPCC are shown in bold



340 type. The lowest values of the sample standard deviation of the PPCC values, denoted  $\hat{s}$ ,  
341 are also shown in bold. Figure 6 illustrates box-plots of the values of PPCC for  
342 distributions fitted to the wet-day series of daily precipitation data at the point and  
343 catchment scales.

344 *[Table 5 goes here]*

345 *[Figure 6 goes here]*

346 Figure 6 and Table 5 indicate that for the wet-day-series of point daily  
347 precipitation depths, all the distributions have median PPCCs well above 0.9, but only the  
348 median PPCCs of G2, P3, and KAP distributions are over 0.99. The same situation  
349 appears in the catchment scale precipitation, except that the median PPCCs of the  
350 remaining four distributions are significantly lower than the corresponding values for  
351 point precipitation.

352 The insets in Figure 6 show detailed views of the boxplots of PPCC values for the  
353 G2, P3, and KAP distributions for point and areal average daily precipitation. From  
354 Figure 6a, KAP distribution results in the best goodness-of-fit for point precipitation  
355 because all of its indices are the best, while the P3 distribution generally performs better  
356 than the G2 distribution. However, for catchment-scale precipitation (Figure 6b), the  
357 four parameter KAP distribution is no longer competitive, and both the G2 and P3 pdfs  
358 will suffice. We are reluctant to advocate the use of a four-parameter pdf, such as the  
359 KAP distribution, due to its inherent complexity, though such a pdf may be needed for  
360 point values as evidenced from our analyses.

#### 361 **4.2.2 Graphical comparison of P3, G2, and KAP**

362 Across all previous comparisons, the P3, G2, and KAP are the best fitting distributions  
363 for describing daily precipitation at the point or catchment scales. The insets in Figure 6  
364 identify the distributions that exhibit the best fit to the each observed series. However,  
365 these inserts do not indicate by how much the best performing distribution outperforms  
366 the second or third best. For this purpose, pairwise comparisons of the PPCC values of  
367 two highly performing distributions for all the stations and catchments are instructive. A  
368 simple graphical method can accomplish this goal.

369 Figure 7 compares the PPCC values of the P3 (vertical axis) and G2 (horizontal  
370 axis) distributions for point- and catchment-scale daily precipitation. Approximately  
371 98% of stations are displayed on the figure; the remaining points lie outside the plot  
372 domains. Points lying above the diagonal line indicate that the P3 distribution has a  
373 higher PPCC for that particular station, and points lying below the diagonal line indicate  
374 the G2 results in a higher PPCC. Figure 7a shows that in nearly every case, the P3  
375 distribution outperforms the G2 distribution. When the G2 does outperform the P3, the  
376 PPCCs are both very high and nearly equal. The point-scale precipitation plot shows that  
377 the P3 distribution performs significantly better than the G2 distribution in many cases.  
378 Thus, we conclude the P3 distribution better represents wet-day daily point precipitation  
379 than the more commonly used G2 distribution in nearly every case. Figure 7b compares  
380 the PPCC values of P3 and G2 for the catchment-scale precipitation. The results are  
381 nearly the same as for the point-scale precipitation in the sense that most points are above

382 the diagonal line; while, for a few catchments where G2 does outperform P3, the points  
383 lie on the dividing line, showing only very slight superiority.

384 *[Figure 7 goes here]*

385 Figure 8 displays similar plots comparing the KAP (vertical axis) and P3  
386 (horizontal axis) distribution for point- and catchment-scale daily precipitation. It can be  
387 seen in Figure 8a that the KAP distribution does not always outperform the P3 pdf, as one  
388 might expect given that it has an additional parameter. We are reluctant to advocate the  
389 KAP pdf given its additional model complexity combined with the fact that it does not  
390 appear to provide a uniform improvement, in either case, over the P3 pdf.

391 *[Figure 8 goes here]*

392

## 393 **5. Discussion**

394 From the L-moment diagrams and PPCC comparisons we concluded that KAP can better  
395 capture the tail behavior of point wet-day series, though both P3 and G2 can provide  
396 reasonable approximations in many situations. In contrast, we found that a KAP pdf is  
397 not needed to approximate the behavior of areal average wet-day series, where instead,  
398 either a P3 or G2 model would suffice. In this section, we evaluate the relationship  
399 between these findings and the size of the catchments considered.

400 Figure 9 displays the PPCC values of P3 and G2 pdfs versus catchment drainage  
401 area for areal average wet-day series. The PPCC values are chosen from 0.99-1,  
402 approximately 96% of catchments are displayed on the figure; the remaining points lie  
403 outside the plot domains. It can be seen that for most of the catchments, the PPCC values  
404 for G2 and P3 pdfs are very close, with points corresponding to G2 and P3 pdfs almost  
405 overlapping. This is especially true for PPCC values higher than 0.998. The phenomena  
406 clearly indicate that when G2 can well represent the behavior of catchment-scale wet-day  
407 precipitation series, P3 also provides very good performance. However, for the areas  
408 where PPCC values are lower than 0.996, the P3 distribution outperforms the G2  
409 distribution for most cases, with a very slight improvement.

410 *[Figure 9 goes here]*

411 Figure 10 shows the spatial map of catchments with the corresponding best  
412 distribution functions for areal average wet-day series. KAP distribution is the best pdf  
413 for large proportion of the catchments especially in the middle of US. P3 distribution  
414 occupies the second large proportion of the catchments especially in east-central US.  
415 Only a very few catchments can be best represented by G2 distribution. Seen from  
416 Figure 10, it seems that the performances of the three pdfs vary greatly. However, as we  
417 have seen from previous figures, the differences between the three pdfs for catchments  
418 are very small.

419 *[Figure 10 goes here]*

## 420 **6. Conclusions**

421 This study has demonstrated that L-moment diagrams and probability plot correlation  
422 coefficient goodness of fit evaluations can provide new insight into the distribution of

423 very long series of daily wet-day precipitation at both the point and catchment scales.  
424 Although previous studies have claimed that the commonly used 2-parameter Gamma  
425 distribution performs fairly well on the basis of traditional goodness-of-fit tests, this  
426 study reveals, through the use of L-moment diagrams and probability plot correlation  
427 coefficient goodness of fit evaluations that very long series of uncensored daily point and  
428 areal average precipitation are better approximated by a KAP distribution and a Pearson-  
429 III distribution respectively, and importantly, they do not resemble any of the other  
430 commonly used distributions. Analogous to the recent study by Papalexiou and  
431 Koutsoyiannis (2016), our evaluations yield very different conclusions than previous  
432 research on this subject and thus could have important implications in climate change  
433 investigations and other studies which employ a pdf of daily precipitation.

434 We conclude that for representing wet-day precipitation, the Gamma and Pearson-  
435 III distributions are comparable with the 4-parameter Kappa distribution for the areal  
436 average precipitation; however, when the point precipitation is of concern, the Kappa  
437 distribution should be the distribution of choice. We also conclude that future  
438 investigations should consider comparisons between the generalized Gamma distribution  
439 introduced by Papalexiou and Koutsoyiannis (2012, 2016) for wet-day daily precipitation  
440 and the G2, Pearson type III and Kappa distributions recommended here.

441 Once analytical and polynomial L-moment relationships and parameter estimation  
442 methods become available for the GG distribution, future studies should compare the P3  
443 and GG distributions on wet-day series, because on the basis of this study, and  
444 Papalexiou and Koutsoyiannis (2016), the P3 and GG distributions appear to have  
445 tremendous potential for approximating the distribution of wet-day series.

446

447

## 448 **Acknowledgements**

449 The first and third authors are partially supported by the National Natural Science  
450 Foundation of China (No. 91547116, 51709033, 91647201). Special thanks are given to  
451 Dr. Simon M. Papalexiou and other two anonymous reviewers and editors for their  
452 constructive remarks.  
453

## 454 **References**

- 455 Blum, A. G., Archfield, S. A., and Vogel, R. M.: On the probability distribution of daily  
456 streamflow in the United States, *Hydrology and Earth System Sciences*, 21, 3093, 2017.
- 457 Bonnin, G. M., Martin, D., Lin, B., Parzybok, T., Yekta, M., and Riley, D.: Precipitation-  
458 frequency atlas of the United States, NOAA atlas, 14, 2006.
- 459 Buishand, T. A.: Some remarks on the use of daily rainfall models, *Journal of Hydrology*,  
460 36, 295-308, 1978.
- 461 Burgueno, A., Martinez, M. D., Lana, X., and Serra, C.: Statistical distributions of the  
462 daily rainfall regime in Catalonia (northeastern Spain) for the years 1950–2000,  
463 *International Journal of Climatology*, 25, 1381-1403, 2005.
- 464 Chen, J., and Brissette, F. P.: Stochastic generation of daily precipitation amounts: review  
465 and evaluation of different models, *Climate Research*, 59, 189-206, 2014.
- 466 Deidda, R., and Puliga, M.: Sensitivity of goodness-of-fit statistics to rainfall data  
467 rounding off, *Physics and Chemistry of the Earth, Parts A/B/C*, 31, 1240-1251, 2006.
- 468 Duan, J., Sikka, A. K., and Grant, G. E.: A comparison of stochastic models for  
469 generating daily precipitation at the HJ Andrews Experimental Forest, 1995.
- 470 Duan, Q., Schaake, J., Andreassian, V., Franks, S., Goteti, G., Gupta, H. V., Gusev, Y.  
471 M., Habets, F., Hall, A., and Hay, L.: Model Parameter Estimation Experiment (MOPEX):  
472 An overview of science strategy and major results from the second and third workshops,  
473 *Journal of Hydrology*, 320, 3-17, 2006.
- 474 Easterling, D. R., Evans, J., Groisman, P. Y., Karl, T. R., Kunkel, K. E., and Ambenje, P.:  
475 Observed variability and trends in extreme climate events: a brief review, *Bulletin of the*  
476 *American Meteorological Society*, 81, 417-425, 2000.
- 477 Geng, S., de Vries, F. W. P., and Supit, I.: A simple method for generating daily rainfall  
478 data, *Agricultural and Forest Meteorology*, 36, 363-376, 1986.
- 479 Groisman, P. Y., Karl, T. R., Easterling, D. R., Knight, R. W., Jamason, P. F., Hennessy,  
480 K. J., Suppiah, R., Page, C. M., Wibig, J., and Fortuniak, K.: Changes in the probability  
481 of heavy precipitation: important indicators of climatic change, in: *Weather and Climate*  
482 *Extremes*, Springer, 243-283, 1999.
- 483 Hershfield, D. M.: Rainfall frequency atlas of the United States for durations from 30  
484 minutes to 24 hours and return periods from 1 to 100 years, 1961.

485 Hosking, J. R.: L-moments: analysis and estimation of distributions using linear  
486 combinations of order statistics, *Journal of the Royal Statistical Society. Series B*  
487 (Methodological), 105-124, 1990.

488 Hosking, J. R.: The four-parameter kappa distribution, *IBM Journal of Research and*  
489 *Development*, 38, 251-258, 1994.

490 Hosking, J. R. M., and Wallis, J. R.: *Regional frequency analysis: an approach based on*  
491 *L-moments*, Cambridge University Press, 1997.

492 Karl, T. R., and Knight, R. W.: Secular trends of precipitation amount, frequency, and  
493 intensity in the United States, *Bulletin of the American Meteorological Society*, 79, 231-  
494 241, 1998.

495 Kigobe, M., McIntyre, N., Wheeler, H., and Chandler, R.. Multi-site stochastic modelling  
496 of daily rainfall in Uganda. *Hydrological sciences journal*, 56, 17-33, 2011.

497 Lee, S. H., and Maeng, S. J.: Frequency analysis of extreme rainfall using L moment,  
498 *Irrigation and Drainage*, 52, 219-230, 2003.

499 Li, Z., Brissette, F., Chen, J.. Finding the most appropriate precipitation probability  
500 distribution for stochastic weather generation and hydrological modelling in Nordic  
501 watersheds. *Hydrological Processes*, 27: 3718-3729, 2013.

502 Madsen, H., Lawrence, D., Lang, M., Martinkova, M., and Kjeldsen, T.: Review of trend  
503 analysis and climate change projections of extreme precipitation and floods in Europe,  
504 *Journal of Hydrology*, 519, 3634-3650, 2014.

505 Mehrotra, R., Srikanthan, R., and Sharma, A.: A comparison of three stochastic multi-site  
506 precipitation occurrence generators, *Journal of Hydrology*, 331, 280-292, 2006.

507 Naghavi, B., and Yu, F. X.: Regional frequency analysis of extreme precipitation in  
508 Louisiana, *Journal of Hydraulic Engineering*, 121, 819-827, 1995.

509 Papalexiou, S. M., and Koutsoyiannis, D.: Entropy based derivation of probability  
510 distributions: A case study to daily rainfall, *Advances in Water Resources*, 45, 51-57,  
511 2012.

512 Papalexiou, S. M., and Koutsoyiannis, D.: Battle of extreme value distributions: A global  
513 survey on extreme daily rainfall, *Water Resources Research*, 49, 187-201, 2013.

514 Papalexiou, S. M., and Koutsoyiannis, D.: A global survey on the seasonal variation of  
515 the marginal distribution of daily precipitation, *Advances in Water Resources*, 94, 131-  
516 145, 2016.

517 Papalexiou, S. M., Markonis, Y., Lombardo, F., AghaKouchak, A., and Foufoula-  
518 Georgiou, E.: Precise temporal Disaggregation Preserving Marginals and Correlations  
519 (DiPMaC) for stationary and nonstationary processes. *Water Resources Research*, 54,  
520 2018. [https:// doi.org/10.1029/2018WR022726](https://doi.org/10.1029/2018WR022726)

521 Park, J.-S., and Jung, H.-S.: Modelling Korean extreme rainfall using a Kappa  
522 distribution and maximum likelihood estimate, *Theoretical and Applied Climatology*, 72,  
523 55-64, 2002.

524 Pilon, P. J., Adamowski, K., and Alila, Y.: Regional analysis of annual maxima  
525 precipitation using L-moments, *Atmospheric Research*, 27, 81-92, 1991.

526 Schoof, J. T., Pryor, S. C., and Surprenant, J.: Development of daily precipitation  
527 projections for the United States based on probabilistic downscaling, *Journal of*  
528 *Geophysical Research: Atmospheres*, 115, D13, 2010.

529 Shoji, T., and Kitaura, H.: Statistical and geostatistical analysis of rainfall in central Japan,  
530 *Computers & Geosciences*, 32, 1007-1024, 2006.

531 Srikanthan, R., and McMahon, T.: Stochastic generation of annual, monthly and daily  
532 climate data: A review, *Hydrology and Earth System Sciences Discussions*, 5, 653-670,  
533 2001.

534 Stedinger, J. R., R.M. Vogel and E. Foufoula-Georgiou: Frequency analysis of extreme  
535 events, *Handbook of Hydrology*, Chapter 18, McGraw Hill Book Co, D.R. Maidment -  
536 editor in chief, 1993..

537 Thom, H. C.: A frequency distribution for precipitation, *Bulletin of the American*  
538 *Meteorological Society*, 32, 397, 1951.

539 Trenberth, K. E.: Changes in precipitation with climate change, *Climate Research*, 47,  
540 123-138, 2011.

541 Vogel, R. M., and Fennessey, N. M.: L moment diagrams should replace product moment  
542 diagrams, *Water Resources Research*, 29, 1745-1752, 1993.

543 Vogel, R. W., and McMartin, D. E.: Probability Plot Goodness-of-Fit and Skewness  
544 Estimation Procedures for the Pearson Type 3 Distribution, *Water resources research*, 27,  
545 3149-3158, 1991.

546 Waggoner, P.E., 1989: Anticipating the frequency distribution of precipitation if climate  
547 change alters its mean, *Agricultural and Forest Meteorology*, 47, 321 – 337.

548 Watterson, I., and Dix, M.: Simulated changes due to global warming in daily  
549 precipitation means and extremes and their interpretation using the gamma distribution,  
550 *Journal of Geophysical Research: Atmospheres*, 108, 2003.

551 Watterson, I. G.: Simulated changes due to global warming in the variability of  
552 precipitation, and their interpretation using a gamma-distributed stochastic model,  
553 *Advances in Water Resources*, 28, 1368-1381, 2005.

554 Waymire, E., and Gupta, V. K.: The mathematical structure of rainfall representations: 1.  
555 A review of the stochastic rainfall models, *Water resources research*, 17, 1261-1272,  
556 1981.

557 Wilby, R. L., and Wigley, T.: Future changes in the distribution of daily precipitation  
558 totals across North America, *Geophysical Research Letters*, 29, 2002.

559 Wilks, D. S.: Maximum likelihood estimation for the gamma distribution using data  
560 containing zeros, *Journal of Climate*, 3, 1495-1501, 1990.

561 Wilks, D. S.: Multisite generalization of a daily stochastic precipitation generation model,  
562 *Journal of Hydrology*, 210, 178-191, 1998.

- 563 Wilks, D. S., and Wilby, R. L.: The weather generation game: a review of stochastic  
564 weather models, *Progress in physical geography*, 23, 329-357, 1999.
- 565 Wilson, P. S., and Toumi, R.. A fundamental probability distribution for heavy rainfall.  
566 *Geophysical Research Letters*, 32, L14812, 2005.
- 567 Woolhiser, D. A., and Roldan, J.: Stochastic daily precipitation models: 2. A comparison  
568 of distributions of amounts, *Water resources research*, 18, 1461-1468, 1982.
- 569 Yoo, C., Jung, K. S., and Kim, T. W.: Rainfall frequency analysis using a mixed Gamma  
570 distribution: evaluation of the global warming effect on daily rainfall, *Hydrological  
571 Processes*, 19, 3851-3861, 2005.

## 572 **Table captions:**

- 573 **Table 1:** Review of literature pertinent to daily precipitation probability distribution  
574 selection.
- 575 **Table 2:** Table 2: Theoretical probability distributions presented on the L-Kurtosis vs L-  
576 Skew L-moment diagram.
- 577 **Table 3:** Theoretical probability distributions presented on the L-Cv vs L-Skew L-  
578 moment diagram.
- 579 **Table 4:** Distributions used in probability plot goodness of fit evaluations.
- 580 **Table 5:** Central tendency and spread of values of PPCC for the 237 precipitation  
581 stations 305 areal average precipitation catchments.

## 582 **Figure captions:**

- 583 **Figure 1:** Map showing locations of a) 237 precipitation gaging stations, and b) 305  
584 catchments.
- 585 **Figure 2:** Distribution of full record length of point precipitation base on weather stations.
- 586 **Figure 3:** Distribution of wet-day record length: a) point precipitation; and b) areal  
587 average precipitation over watersheds. Days with zero precipitation are removed in the  
588 wet-day records
- 589 **Figure 4:** L-Cv vs L-Skew L-moment ratio diagram of sample L-moments and  
590 theoretical distributions: a) point precipitation; and b) areal average precipitation depths.
- 591 **Figure 5:** L-Skew vs L-Kurtosis L-moment ratio diagram of sample L-moments and  
592 theoretical distributions: a) point precipitation; and b) areal average precipitation depths.  
593 Logistic (L), Normal (N), Uniform (U), Gumbel (G), and Exponential (E) distributions  
594 appear as a single point.
- 595 **Figure 6:** Standard boxplots of  $r$  for all 7 distributions evaluated for wet-day series of a)  
596 point precipitation, and b) areal average precipitation depths.
- 597 **Figure 7:** Comparison of PPCC ( $r$ ) values for the P3 (vertical axis) and G2 (horizontal  
598 axis) distributions for the a) point, and b) areal average precipitation depths series. Points  
599 lying above the line represent stations with a higher  $r$  for the P3 distribution than G2  
600 distribution.

601 **Figure 8:** Comparison of r values for P3 (horizontal axis) and KAP (vertical axis)  
602 distributions for the a) point and b) areal average precipitation depths' wet-day series.

603 **Figure 9:** The spatial distribution of best daily precipitation distribution function.

604 **Figure 10:** The spatial map of catchments with the corresponding best distribution  
605 functions for areal average wet-day series.

606



607 **Tables**

608

**Table 1:** Review of literature pertinent to daily precipitation probability distribution selection.

<i>1. Stochastic Precipitation Modelling:</i>						
<b>Author</b>	<b>Year</b>	<b>Stations</b>	<b>Series type</b>	<b>Duration</b>	<b>Distribution</b>	<b>Justification</b>
Thom	1951		Wet-day	1-day	Gamma	
Buishand	1978	6	Wet-day	1-day	Gamma	Cv-Cs ratio
Geng et al	1986	6	Wet-day, by month	1-day, monthly	Gamma	Regress. fit: $\beta$ vs mean wet-day depth
Woolhiser and Roldan	1982		Wet-day	1-day	Mixed Exponential	MLE, Akaike Information Criterion
Duan et al	1995	1	Wet-day, by month	1-day	Calib. W2, Gamma	MLE, Chi-sq test
Wilks	1998	25	Wet-day	1-day	Mixed Exponential	MLE, goodness of fit
Waterson and Dix	2003		Wet-day	1-day	Gamma	Literature
Burgueno et al	2005	75	Wet-day	1-day	Exponential, Weibull	Normalized Rainfall Curve
Kigobe et al	2011	110	Wet-day, by month		Gamma	
Li et al	2013	24	Wet-day	1-day	Mixed Exponential	Goodness of fit and Kolmogorov–Smirnov tests
Schoof	2015	Grided precipitation	Wet-day	1-day	Gamma	Goodness of fit
<i>2. Precipitation Frequency Analysis</i>						
<b>Author</b>	<b>Year</b>	<b>Stations</b>	<b>Series type</b>	<b>Duration</b>	<b>Distribution</b>	<b>Justification</b>
Hershfield (TP-40)	1962		AMS	24 hour	Gumbel	
Pilon et al	1991	75	AMS	5 min - 24 hour	GEV	L-moments
Naghavi & Yu	1995	25	AMS	1-24 hour	GEV	L-moments, PWMs, Monte Carlo experiments
Park and Jung	2002	61	AMS	1, 2-day	Kappa(4)	
Lee and Maeng	2003	38	AMS	1-day	GEV, GLO	L-moments
Bonnin et al	2006		AMS	5 min - 24 hour	GEV	L-moments
Shoji and Kitaura	2006	243	Complete, Wet-day	Hour, Day, Month, Year	Lognormal, Weibull	Goodness of fit
Deidda and Puliga	2006	200	Left Censored Wet-day PDS	1-day	Generalized Pareto	“Failure-to-reject” method, L-moments
Wilson and Toumi	2005	270	Complete	1-day	Self-derived	
Papalexioi and Koutsoyiannis	2012	11,519	Wet-Day	1-day	Generalized Gamma	L-moments
Papalexioi and Koutsoyiannis	2013	15,137	AMS	1-day	GEV	L-moments
Papalexioi and Koutsoyiannis	2016	14,157	Wet-Day, by month	1-day	Generalized Gamma and Burr type XII	L-moments and Goodness-of-fit
Papalexioi et al	2018	GCM	Wet-Day, by month	1-month	Generalized Gamma	L-moments

3. Precipitation Trends and Climate Change

<b>Author</b>	<b>Year</b>	<b>Stations</b>	<b>Series type</b>	<b>Duration</b>	<b>Distribution</b>	<b>Justification</b>
Waggoner	1989	55	Monthly	1-month	Gamma	Literature Review
Groisman et al	1999	1313	Summer (wet-day)	1-day	Gamma	Literature Review, goodness of fit to extreme rainfall quantiles
Wilby and Wigley	2002	GCM	Seasonal	1-day	Gamma	Literature Review
Yoo et al	2005	31	Monthly (wet-day)	1-day	Gamma	Literature Review
Watterson	2005	GCM	January, July	1-month (daily forced)	Gamma	Literature Review

**Table 2:** Theoretical probability distributions presented on the L-Kurtosis vs L-Skew L-moment diagram.

Distribution	Abbreviation	PDF	Parameters
Kappa	KAP	$F(x) = \left\{ 1 - \gamma_2 \left[ 1 - \gamma_1 (x - \alpha) / \beta \right]^{1/\gamma_1} \right\}^{1/\gamma_2}$ $f(x) = \beta^{-1} \left[ 1 - \gamma_1 (x - \alpha) / \beta \right]^{(1/\gamma_1) - 1} \times [F(x)]^{1 - \gamma_2}, \beta > 0$	4
Generalized Extreme Value Type III	GEV	$f(x) = \frac{1}{\beta} \left( 1 + \gamma \frac{x - \alpha}{\beta} \right)^{-1/\gamma - 1} \exp \left[ - \left( 1 + \gamma \frac{x - \alpha}{\beta} \right)^{-1/\gamma} \right]$	3
Generalized Logistic	GLO	$f(x) = \frac{\gamma \exp(-\frac{x - \alpha}{\beta})}{\beta \left( 1 + \exp(-\frac{x - \alpha}{\beta}) \right)^{\gamma + 1}}$	3
Generalized Pareto	GPA	$f(x) = \frac{1}{\beta} \left( 1 + \frac{\gamma(x - \alpha)}{\beta} \right)^{-1/\gamma - 1}$	3
Lognormal	LN3	$f(x) = \frac{1}{(x - \gamma)\sqrt{2\pi\beta}} \exp \left[ -\frac{1}{2} \left( \frac{\ln(x - \gamma) - \alpha}{\beta} \right)^2 \right]$	3
Pearson Type III	P3	$f(x) = \frac{1}{\beta^\gamma \Gamma(\gamma)} (x - \alpha)^{\gamma - 1} \exp(-\frac{x - \alpha}{\beta})$	3
Exponential	E	$f(x) = \begin{cases} \lambda \exp(-\lambda x), & x \geq 0 \\ 0, & x < 0 \end{cases}$	2
Gumbel	G	$f(x) = \frac{1}{\beta} \exp \left[ \frac{x - \alpha}{\beta} - \exp\left(\frac{x - \alpha}{\beta}\right) \right]$	2
Normal	N	$f(x) = \frac{1}{\sqrt{2\pi\beta^2}} \exp\left(-\frac{(x - \alpha)^2}{2\beta^2}\right)$	2
Logistic	L	$f(x) = \frac{\exp(-\frac{x - \alpha}{\beta})}{\beta \left( 1 + \exp(-\frac{x - \alpha}{\beta}) \right)^2}$	2
Uniform	U	$f(x) = \begin{cases} \frac{1}{b - a}, & a < x < b \\ 0, & x < a \text{ or } x > b \end{cases}$	1

Note that  $\alpha, \beta, \gamma$  are parameters used for location, scale, and shape, respectively; if more than one parameter of the same type exists, indices (e.g.  $\gamma_1, \gamma_2$ ) are used.

**Table 3:** Theoretical probability distributions presented on the L-Cv vs L-Skew L-moment diagram.

Distribution	Abbreviation	PDF	Parameters
--------------	--------------	-----	------------

Gamma	G2	$f(x) = \frac{x^{\gamma-1} \exp(-\frac{x}{\beta})}{\Gamma(\gamma) \beta^\gamma}$	2
Generalized Pareto	GP2	$f(x) = \frac{1}{\beta} \left(1 + \frac{\gamma x}{\beta}\right)^{-(1/\gamma-1)}$	2
Lognormal	LN2	$f(x) = \frac{1}{x\beta\sqrt{2\pi}} \exp\left(-\frac{(\ln x - \alpha)^2}{2\beta^2}\right)$	2
Weibull	W2	$f(x) = \frac{\gamma}{\beta} \left(\frac{x}{\beta}\right)^{\gamma-1} \exp\left[-\left(\frac{x}{\beta}\right)^\gamma\right], \quad x \geq 0$	2

Note that  $\alpha$ ,  $\beta$ ,  $\gamma$  are used for location, scale, and shape, respectively; if more than one parameter of the same type exists, indices (e.g.  $\gamma_1$ ,  $\gamma_2$ ) are used.

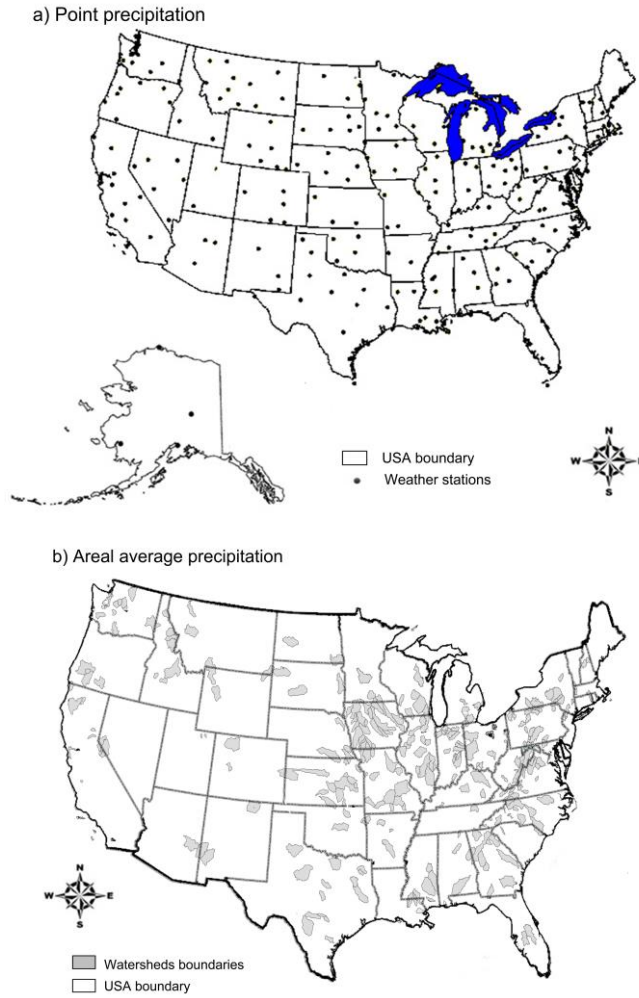
**Table 4:** Distributions used in probability plot goodness of fit evaluations.

Distribution	Abbreviation	Parameters
Generalized Extreme Value Type III	GEV	3
Generalized Logistic	GLO	3
Generalized Pareto	GPA	3
Lognormal	LN3	3
Pearson Type III	P3	3
Gamma	G2	2
Kappa	KAP	4

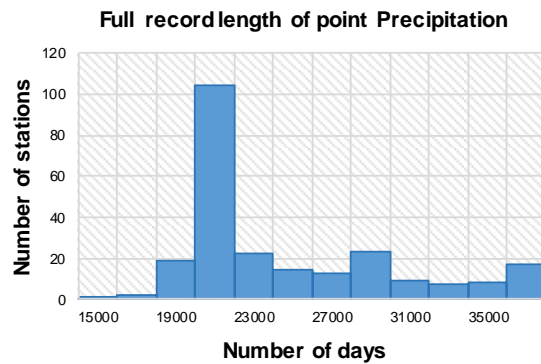
**Table 5:** Central tendency and spread of values of PPCC for the 237 precipitation stations and 305 catchments.

Distribution	Point precipitation			Percentiles		Areal average precipitation			Percentiles	
	Mean	Median	$\hat{s}$	95th	5th	Mean	Median	$\hat{s}$	95th	5th
P3	0.9952	0.9971	0.0063	0.9995	0.9872	<b>0.9977</b>	0.9985	<b>0.0028</b>	0.9996	<b>0.9936</b>
GEV	0.9338	0.9375	0.0222	0.9609	0.8944	0.8003	0.7965	0.0474	0.8917	0.7264
GPA	0.9793	0.9828	0.0145	0.9949	0.9500	0.8688	0.8687	0.0484	0.9586	0.7894
GLO	0.9115	0.9154	0.0235	0.9423	0.8734	0.7800	0.7750	0.0441	0.8669	0.7101
LN3	0.9838	0.9855	0.0075	0.9924	0.9727	0.9362	0.9373	0.0224	0.9737	0.8983
G2	0.9925	0.9949	0.0079	0.9990	0.9789	0.9974	0.9985	0.0034	0.9996	0.9924
KAP	<b>0.9971</b>	<b>0.9985</b>	<b>0.0048</b>	<b>0.9997</b>	<b>0.9915</b>	0.9976	<b>0.9987</b>	0.0026	<b>0.9998</b>	0.9929

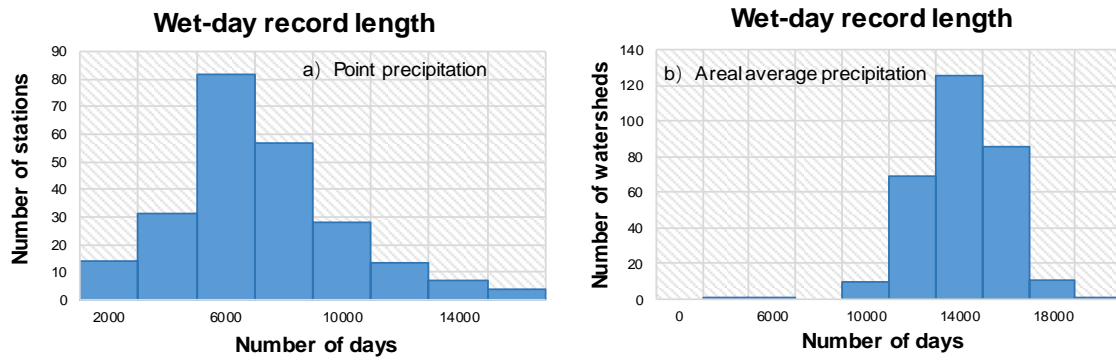
# Figures



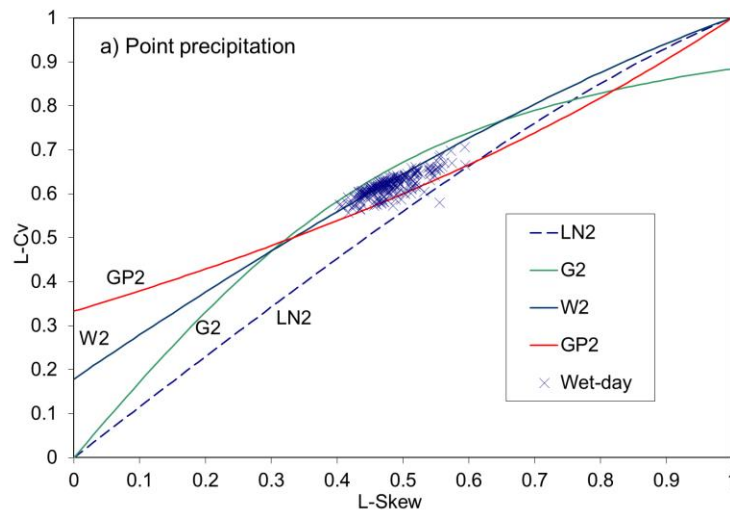
**Figure 1:** Map showing locations of a) 237 point precipitation gaging stations, and b) 305 MOPEX catchments.

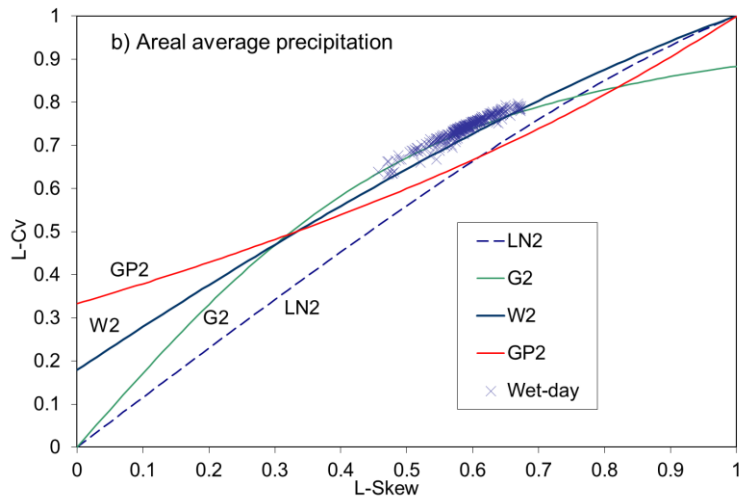


**Figure 2:** Distribution of length of records of point daily precipitation data for the 237 gaging stations depicted in Figure 1a.

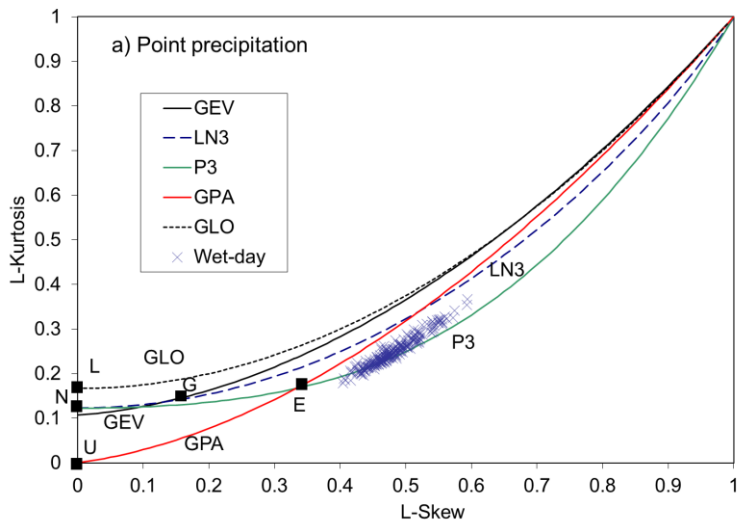


**Figure 3:** Distribution of wet-day record lengths corresponding to the two datasets: a) point precipitation; and b) areal average precipitation over catchments. Days with zero precipitation are removed in the wet-day records





**Figure 4:** L-Cv vs L-Skew L-moment ratio diagram of sample L-moments and theoretical distributions for: a) point daily precipitation; and b) areal average daily precipitation depths.





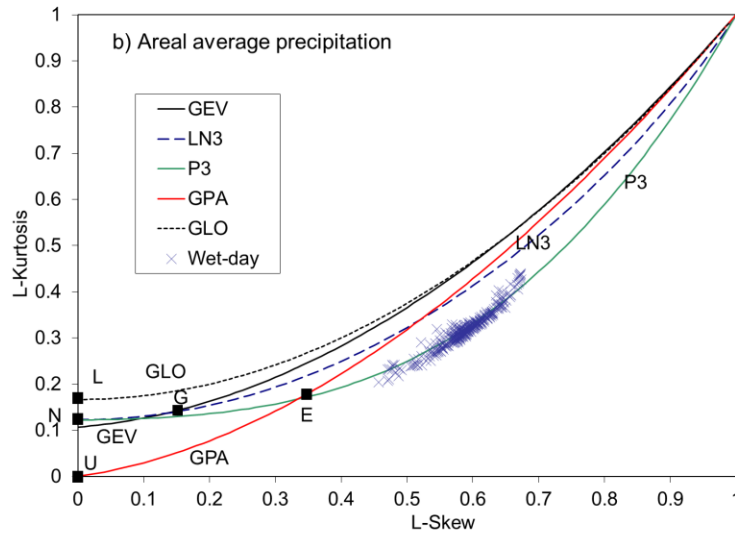


**Figure 5:** L-Skew vs L-Kurtosis L-moment ratio diagram of sample L-moments and theoretical distributions for: a) point daily precipitation; and b) areal average daily precipitation depths. Note that Logistic (L), Normal (N), Uniform (U), Gumbel (G), and Exponential (E) distributions appear as a single point.

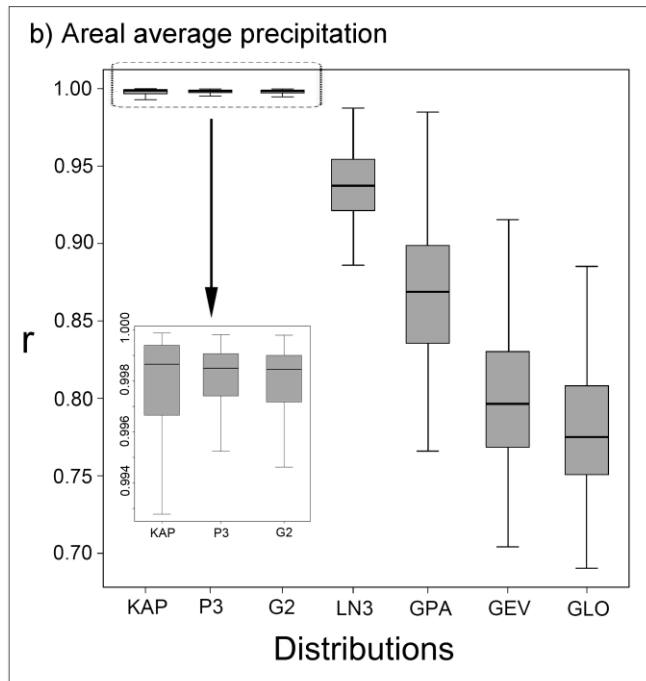
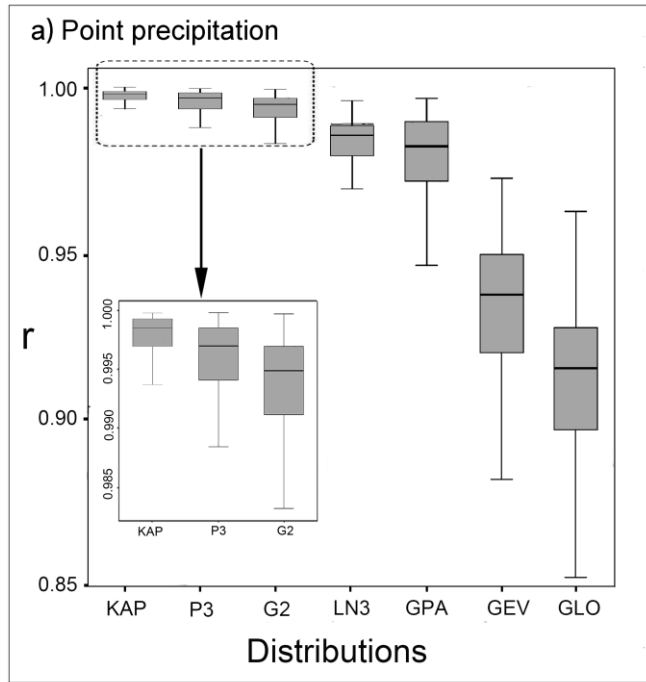


**Figure 6:** Standard boxplots of  $r$  for all 7 distributions evaluated for wet-day series of a) point precipitation, and b) areal average precipitation depths.

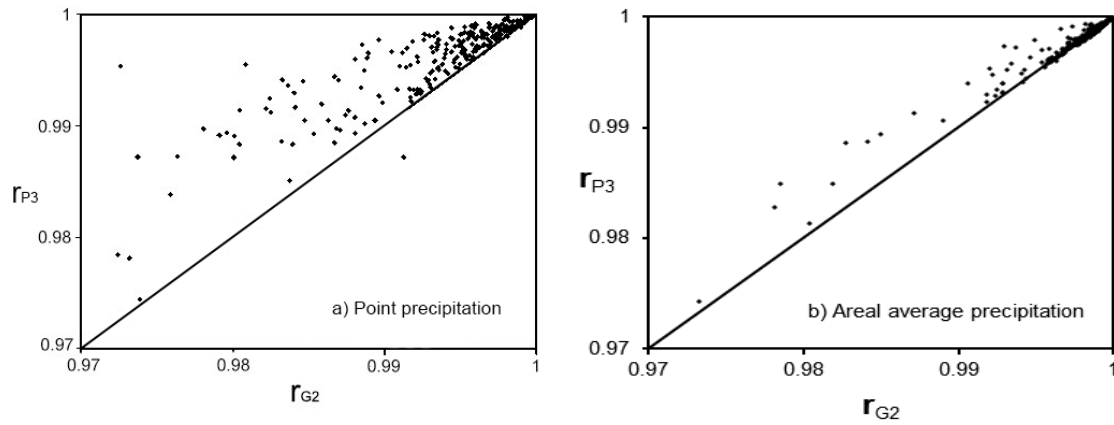


**Figure 7:** Comparison of PPCC ( $r$ ) values for the P3 (vertical axis) and G2 (horizontal axis) distributions for the a) point, and b) areal average precipitation depths series. Points lying above the line represent stations with a higher  $r$  for the P3 distribution than G2 distribution.

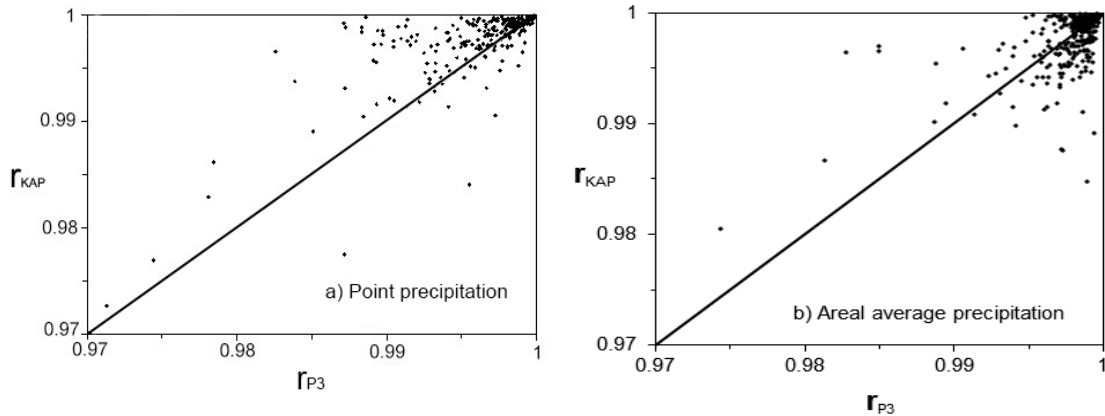


**Figure 8:** Comparison of  $r$  values for P3 (horizontal axis) and KAP (vertical axis) distributions for the a) point and b) areal average precipitation depths' wet-day series.

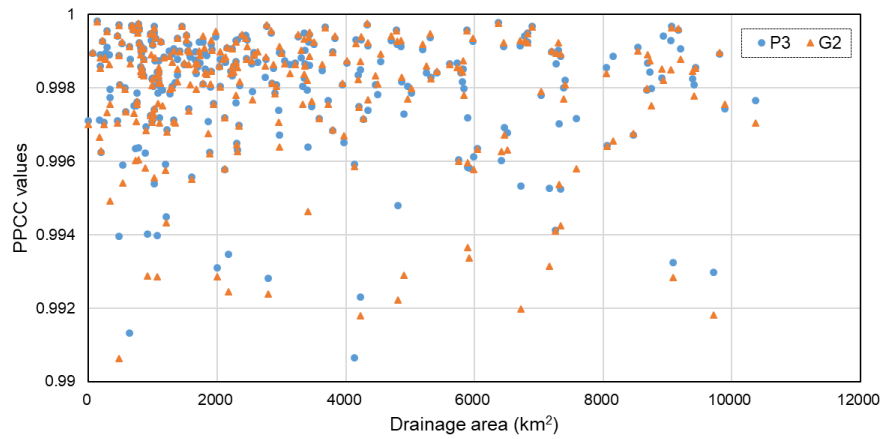


**Figure 9:** the PPCC values of P3 and G2 pdfs versus catchment drainage area for areal average wet-day series.

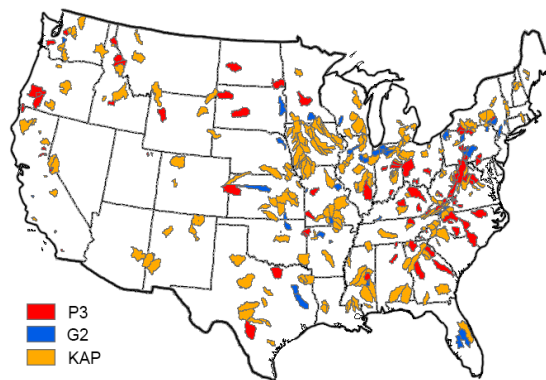


**Figure 10:** The spatial map of catchments with the corresponding best distribution functions for areal average wet-day series.